International Journal of Biological Macromolecules 371 (2026) 152886

Contents lists available at ScienceDirect

International Journal of Biological Macromolecules

journal homepage: www.elsevier.com/locate/ijbiomac

Sustainable carboxymethyl cellulose from palm flower agro-waste as a bio-dielectric material for electronic devices

Sunarkani Ganesh [a], K. Vijaya Bhaskar Reddy [a], K. Chaithanya [a], Sagar Dnyandev Patil [b], T. Senthil Vadivel [c], R. Mallikarjun [d], Sunesh Narayanaperumal [e,*], Indran Suyambulingam [e,*], Sivarao Subramonian [f], Siva Avudaiappan [g]

[a] Department of Mechanical Engineering, Marri Laxman Reddy Institute of Technology and Management (MLRITM), Hyderabad, 500043, Telangana, India
[b] Mechanical Engineering Department, Sharad Institute of Technology College of Engineering, Kolhapur, 416115, Maharashtra, India
[c] Department of Civil Engineering, School of Engineering and Technology, Manav Rachna International Institute of Research and Studies, Faridabad, 121004, Haryana, India
[d] Department of Electronics and Communications, Alliance University, Bengaluru, 562106, Karnataka, India
[e] Centre of Excellence–Advanced Materials Synthesis (CoE-AMS), AU-STIC, Department of Mechanical Engineering, Alliance School of Applied Engineering, Alliance University, Bengaluru, 562106, Karnataka, India
[f] Faculty of Industrial and Manufacturing Technology and Engineering, Universiti Teknikal Malaysia Melaka, 76100, Melaka, Malaysia
[g] Departamento de Ciencias de La Construcción, Facultad de Ciencias de La Construcción y Ordenamiento Territorial, Universidad Tecnológica Metropolitana, Santiago, Chile

ARTICLE INFO

Keywords:
Carboxymethyl cellulose
Borassus flabellifer
Agro-waste valorization
Degree of substitution
Sustainable biopolymers
Cellulose derivatives

ABSTRACT

Carboxymethyl cellulose (CMC) was first synthesized using *Borassus flabellifer* flower agro-waste, which is non-food and mostly discarded floral biomass. CMC is extracted via alkali treatment, bleaching, and alkalization with sodium chloroacetate. This article seeks to show how palm flower residues can be transformed into useful cellulose derivatives for sustainable material production. This method yielded 70.3 ± 1.8% CMC with a density of 0.48 ± 0.03 g/cm^3 and a neutral pH. Chemical analysis revealed that the carboxyl content was 21.8 ± 0.9% and the degree of substitution was 0.78 ± 0.04%, leading to efficient carboxymethylation. The Fourier transform infrared spectrum showed typical carboxylate peaks at 1562, 1447, and 1348 cm^{-1}, and XRD showed a semi-crystalline structure with a crystallinity index of 48.6% and a crystallite size of about 4.2 nm. SEM and particle size analyses revealed that it exhibits a unique multiscale fibrous-flaky morphology (~0.067 mm), which justifies its applicability in biodegradable and sustainable material systems. In addition, CMC pellets were synthesized, and their electrical properties were tested. The analysis of the DC measurement indicated a leakage current of 8.1 μA at an applied voltage of 20 *V*, whereas the AC impedance study displayed a loss tangent of 0.87. The dielectric analysis revealed moderate insulating behavior with a leakage current of 8.1 μA at 20 V and a relatively high loss tangent (~0.87). The CMC material shows a moderate dielectric response with characteristics typical of polar biopolymer systems. The observed dielectric loss response indicates applications in low-power and environmentally sustainable electronic applications rather than high-performance energy storage systems.

1. Introduction

The growing environmental liability of petroleum-based polymers, the decline of fossil resources, and strict environmental policies have hindered investigative activities in sustainable, biodegradable, and bio-based polymers [1]. In this regard, polysaccharide-based polymers have attracted considerable interest due to their renewable, abundant, less toxic, and environmentally friendly properties. Carboxymethyl cellulose (CMC) is one of the most industrially important functional biopolymers because of its good water solubility, chemical diversification, film-forming properties, and ability to control rheological properties. CMC is a linear, anionic polysaccharide that is produced by etherifying cellulose hydroxyl groups with carboxymethyl groups [2]. This results in a molecule that is more hydrophilic and easily processed while maintaining the structural strength of cellulose. CMC has found wide use in a large variety of applications, including food formulation thickening

* Corresponding authors.
E-mail addresses: nsunesh16@gmail.com (S. Narayanaperumal), indransdesign@gmail.com (I. Suyambulingam).

https://doi.org/10.1016/j.ijbiomac.2026.152886
Received 19 January 2026; Received in revised form 29 May 2026; Accepted 2 June 2026
Available online 3 June 2026

agents, pharmaceutical binders and controlled drug release matrices, cosmetics viscosity modifiers, paper and textile industry sizing and coating agents, oil-well drilling fluids, adhesives, and is also finding use in biodegradable packaging films, hydrogels, membranes, and composite materials [3]. The flexibility of CMC is achieved because its level of substitution, molecular weight, and the distribution of functional groups can be modified to suit certain application needs. Researchers have reported the synthesis of CMC using rice husk through microwave assistance. They isolated cellulose from rice husk and then transformed this cellulose into CMC, achieving a degree of substitution (DS) of 0.79 under optimal conditions of alkalization and monochloroacetic acid dosage, showing that rice husk can also be used to obtain CMC with a comparable performance to many other common agro-sources. In a study on sugarcane bagasse, CMC with a DS up to 2.41 and purity of about 71.6% was obtained using steam explosion pulping, alkali, and etherification processes, which overall showed that the concentration of NaOH and monochloroacetic acid, as well as reaction parameters, have a considerable influence on optimizing CMC properties in bagasse [4].

Pineapple leaf fibers have also been valorized in recent stages with the isolation of microcrystalline cellulose and converted to carboxymethyl microcrystalline cellulose (CMC-MCC) with elaborate structural and morphological descriptions, reflecting the possibility of high-value biopolymer derivatives from fruit agro-wastes. Likewise, sugarcane leaves were used as an agro-residue lignocellulosic feedstock, producing CMC products with a DS value of between 0.46 and 0.86, with confirmed high purity by Fourier transform infrared (FTIR), X-ray diffraction (XRD), and scanning electron microscopy (SEM) analyses, to be used in the industrial application of CMC as a coated paper filler, textile sizer, and ceramic coating.

Even though agro-residues have been thoroughly studied, many biomass resources in many areas have not been fully used. In particular, large-scale biomass resources may be considered waste because they are not directly used as useful materials. *Borassus flabellifer*, or palmyra palm, is widely grown in South and Southeast Asia, in India, Sri Lanka, and Africa [5]. The plant is traditionally used for its sap, fruits, leaves, and timber, but the flowers of *B. flabellifer* not only produce a lot of agro-waste during their seasonal harvesting and processing. These waste flower residues are usually disposed of or allowed to rot, which causes an environmental nuisance and thus under-exploitation of a potentially useful lignocellulosic resource [6]. Early compositional research shows that the biomass of *B. flabellifer* flower is high in cellulose and hemicellulose, and has a low proportion of lignin, making it a prospective raw material to extract cellulose [7].

The selection of *B. flabellifer* flower agro-waste as a cellulose source is important as it is sustainable, non-food, and abundant in the region. Its relatively low lignin content allows the separation of cellulose with less intense chemical treatment and the subsequent decrease in the severity of the processing and the use of chemicals. Despite these advantages, there is a dearth of research on cellulose recovery and CMC manufacture from *B. flabellifer* flower waste. Research on exploiting palm-based floral agro-wastes as a source of high-value polymers by successive chemical treatments to remove non-cellulosic elements appears to be lacking. B. flabellifer flower flower agro waste based CMC exhibits promising water-retaining agent and rheology modifier in cementitious systems. Hemicellulose is often dissolved by alkali treatment, which also disperses the lignin–carbohydrate complex. The remaining lignin is then dissolved, and the cellulose's purity is improved by bleaching it with oxidizing chemicals such as hydrogen peroxide and sodium hypochlorite. Carboxymethylation of the purified cellulose is then employed using a carboxymethylation process in which the activation step is performed through the alkali solution, mainly sodium hydroxide, followed by the etherification of the cellulose with monochloroacetic acid or sodium monochloroacetic acid [8]. This process creates sodium CMC, which is more water soluble and functional, by adding carboxymethyl groups to the cellulose's backbone. The supply of cellulose, crystallinity, reaction conditions, and the availability of hydroxyl groups all have a significant impact on the degree of substitution, efficacy of carboxymethylation, and final characteristics of CMC.

Although CMC production from cellulose obtained from agro-waste has been largely reported, creating a product with constant quality, sufficient substitution level, and similar functionality to commercial CMC remains a challenge [9]. Moreover, there is incomplete knowledge on the relationship between the biomass source, extraction chemistry, and the final product CMC functional properties, especially from non-conventional feedstock, including palm flower residues. There is also a noticeable lack of systematic investigations that combine cellulose isolation, chemical modification, and full characterization to assess the suitability of such biomass-derived CMC to be a sustainable material source.

The conversion of agricultural residues into value-added biopolymer products, such as CMC, is beneficial for the environment and for better utilization of resources. The valorization of agro-waste will certainly boost the circular economy and the production of sustainable materials. Simultaneously, it will also abate the dumping of biomass and open burning in the field [10]. Cellulose derived from *B. flabellifer* is proposed in this study. CMC, having structural and physicochemical features suitable for sustainable dielectric applications, can be successfully developed from flabellifer flower agro-waste. The investigation of electrical and dielectric properties was carried out to check the feasibility of CMC from agro-wastes to be used as a bio-based dielectric. To assess the suitability of biodegradable and eco-friendly electronic systems, leakage behavior, polarization mechanisms, and frequency-dependent response must be understood. The resulting CMC pellets studied the leakage current from DC measurement and loss tangent from the impedance measurement, indicating moderate dielectric behavior. Although CMC made from different agricultural wastes has been extensively documented, systematic research on its impedance modeling and AC/DC dielectric behavior is still lacking. It is worth noting that bio-based dielectric materials typically have higher dielectric losses than synthetic polymers. Thus, in this study, we investigated the possibility of using CMC from *B. flabellifer* as an environmentally sustainable material for electronic devices.

2. Materials and methods

2.1. Materials used

The agro-waste was *the B. flabellifer* flower, which was gathered locally in Tamil Nadu, India. This study used sodium hydroxide (NaOH, 98%), hydrogen peroxide solution (H_2O_2, approximately 10–12% *w/v*), isopropanol (99%), chloroacetic acid ($ClCH_2COOH$, 99%), ethanol (C_2H_5OH, 99.52%, analytical grade), sodium chloroacetate (CH_2ClCO_2Na), and distilled water. All chemicals used in this study were of analytical reagent (AR) grade and were used as received without further purification.

2.2. Synthesis of CMC

The palm flower agro-waste was used for the synthesis of CMC via cellulose extraction, alkalization, and carboxymethylation. Initially, 50 g of palm flower biomass was washed with distilled water to remove dust and dirt from its surface and dried at 60 °C in an oven for 12 h. Thereafter, the dried material was ground into powder and alkali-treated with 500 mL of 4 wt% NaOH solution at 80 °C for 2 h with continuous stirring. In this step, lignin and hemicellulose were removed. The sample was washed repeatedly until neutralization was reached.

The purified cellulose was obtained by bleaching the delignified material at 70 °C for 1 h using 400 mL of 3 wt% H_2O_2. The cellulose was filtered, washed, and dried at 60 °C to give 20–25 g cellulose. For alkalization, 20 g of the cellulose extract was dispersed in 200 mL isopropanol. A solution containing sodium hydroxide was formed by dissolving 20 g NaOH in 40 mL distilled water slowly with stirring. The

mixture was stirred at room temperature for 1 h to form an alkali with cellulose. Next, 24 g sodium chloroacetate (SMCA) was added to the reaction mixture, and the temperature was increased to 60–65 °C. The reaction mixture was allowed to continue under constant stirring for 3 h for carboxymethylation, where hydroxyl groups of cellulose were substituted by carboxymethyl groups. When the reaction was complete, the mixture was then cooled to room temperature, and CMC was precipitated by the addition of 300 mL of 70% ethanol. The product, which was formed as a precipitate, was filtered and washed several times with ethanol to get rid of sodium chloride and unreacted reagents [11]. The CMC was finally dried at 60 °C for a period of 12–24 h. Further characterization and application of the CMC were carried out after storing it. The extraction methodology of CMC from *B. flabellifer* flower waste is shown in Fig. 1.

2.3. Physical and chemical analyses

The yield of CMC was calculated using the ratio of the dry mass of synthesized CMC to the dry mass of raw material used in the etherification process and expressed as a percentage according to Eq. (1) [12].

$$Yield\% = \frac{W_{CMC}}{W_{BFF}} \times 100 \quad (1)$$

Where W_{CMC} is the dry weight of CMC obtained, and W_{BFF} is the initial dry weight of the extracted *B. flabellifer* flower.

The density was determined following standard powder characterization procedures by gently filling a graduated cylinder with a known mass of dried CMC without tapping and calculating the mass-to-volume ratio using Eq. (2) [13].

$$Density = \frac{m}{v} \quad (2)$$

where m is the mass of CMC (g), and *V* is the occupied *v*olume (cm^3).

Moisture content was measured by oven drying approximately 1 g CMC at 105 °C until constant weight, in accordance with ASTM Standard D1439, and calculated using Eq. (3).

$$MC = \frac{w_i - w_f}{w_i} \times 100 \quad (3)$$

where w_i and w_f are the initial and final weights of the sample, respectively.

The pH of a 1% (*w/v*) aqueous CMC solution was measured at room temperature using a calibrated digital pH meter, following USP guidelines for cellulose derivatives. Solubility was qualitatively assessed by dispersing CMC in distilled water under continuous stirring and observing dissolution behavior and solution clarity [14].

Chemical analysis was performed to determine the carboxyl content of CMC using acid–base titration, following the method described in ASTM D1439 and ISO 5351. Briefly, a known mass of CMC was converted to its acidic form, suspended in distilled water, and titrated with standardized sodium hydroxide solution [15]. The carboxyl content was calculated using Eq. (4):

$$Carboxyl\ content = \frac{V \times N \times 0.058}{W} \times 100 \quad (4)$$

where *V* is the volume of NaOH consumed (mL), *N* is the normality of NaOH, 0.058 is the milliequivalent weight of the carboxymethyl group, and *W* is the mass of the dry CMC sample (g).

The degree of substitution (DS), defined as the average number of hydroxyl groups substituted per anhydroglucose unit of cellulose, was calculated from the carboxyl content, as commonly reported for CMC characterization [16]. The DS is a unitless value ranging from 0 to 3, representing the average number of substituted hydroxyl groups per anhydroglucose unit in the cellulose structure.

2.4. FTIR analysis

To clarify the chemical structure and validate the achievement of the carboxyl methylation of cellulose generated by using *B. flabellifer* flower agro-waste, FTIR spectroscopy was used. The spectra of the extracted cellulose and the synthesized CMC in FTIR were registered with a Bruker Alpha II FTIR spectrometer (Germany) with an attenuated total reflectance accessory [17]. To ensure that the spectra were repeatable, all materials were dried in the oven at 60 °C before being analyzed for moisture. The measurements were conducted with a wavenumber range of 4000–400 cm^{-1} and a spectral resolution of 4 cm^{-1}, and every spectrum was displayed as an average of 32 consecutive scans. The

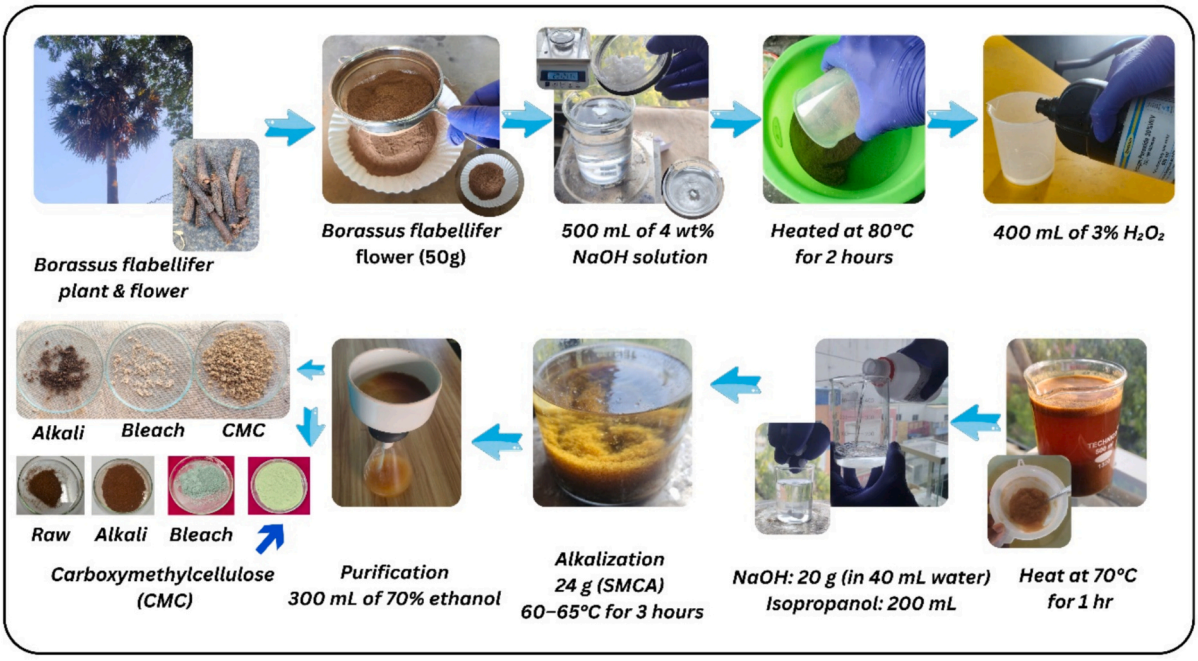

Fig. 1. Extraction methodology of CMC from *B. flabellifer* flower waste.

resulting spectra were interpreted to determine the typical absorption bands related to hydroxyl stretching, ether structures, and carboxylate structures, offering qualitative proof of the structural alteration and formation of CMC.

2.5. XRD analysis

XRD was used to obtain the crystalline structure of the CMC extracted in *B. flabellifer* flower agro-waste. The data were measured using a Bruker D8 Advance X-ray diffractometer, which has Cu-Kα radiation (λ =1.5406 Å) at 40 kV and 40 mA. A 2θ range of 5–50° was scanned in steps of 0.02° and at a scanning rate of 2°/min to compute the peak deconvolution of overlapping crystalline and amorphous peaks using the Gaussian fitting method, mounted on a glass sample holder using powdered CMC samples [18]. The Segal empirical method was used to find the crystallinity index (CI).

$$CI = \frac{I_{200} - I_{am}}{I_{200}} \times 100 \quad (5)$$

where I_{200} is the maximum intensity of the (200) crystalline peak (22° 2θ), and I_{am} is the intensity of the amorphous background (18° 2θ).

The crystallite size (CS) was estimated using the Scherrer equation.

$$CS = \frac{K\lambda}{\beta cos\theta} \quad (6)$$

where K is the shape factor (0.9), λ is the X-ray wavelength (1.5406 Å), β is the full-width at half maximum (FWHM) of the peak measured in radians, and θ is the Bragg diffraction angle [19]. OriginPro 2023 software was used to deconvolute and compute the CS, providing valuable information on the crystallinity and nanoscale sizes of the CMC extracted from *B. flabellifer* [20].

2.6. SEM analysis

The morphology and microstructure of the *B. flabellifer* flower agro-waste on the surface and inside CMC were studied with the help of SEM. It was analyzed using a ZEISS EVO 18 SEM at an accelerating voltage of 5–15 kV under high-vacuum conditions. Before imaging, the dried CMC powder was attached to aluminum stubs with double-sided carbon adhesive tape and sputtered with a thin film (around 10 nm thick) of gold (Quorum Q150R ES sputter coater) to allow electrical conductivity and reduce the charging effects of the surface [21].

2.7. EDS analysis

The *B. flabellifer* flower agro-waste was extracted to produce CMC, and the elemental composition and chemical purity of CMC were determined using energy-dispersive X-ray spectroscopy (EDS) and a scanning electron microscope. It was analyzed with the help of an Oxford Instruments X-Max EDS detector connected to a ZEISS EVO 18 SEM that works at an accelerating voltage of 15 kV [22]. The CMC samples used for SEM analysis were initially subjected to EDS without any further sample modification.

2.8. Particle size analysis

ImageJ software (National Institutes of Health, USA) was used to analyze the size of the extracted CMC particles of *B. flabellifer* based on SEM micrographs. The SEM images were taken at the same magnification and accelerating voltage to achieve the same level of analytical consistency. Before analysis, the images were calibrated with the help of a scale bar incorporated in each micrograph to transform pixel counts of the micrographs into micrometers. The calibrated images were converted into 8-bit grayscale images, and a threshold was applied to delineate the periphery of the particles [23]. The dimensions of the particles were determined using the "Analyze Particles" mode in ImageJ, and at least 25 individual particles were analyzed in each sample to obtain statistically dependable results.

2.9. Surface roughness analysis

ImageJ software was used to analyze the surface morphology images from SEM to examine the surface roughness and topographical features of the extracted CMC from *B. flabellifer* flower agro-waste. The SEM micrographs with a consistent level of magnification were processed with the surface plot and line profile features of ImageJ [24]. Each pixel was chosen using several regions of interest to minimize small variances and get representative surface data. Other surface characteristics to evaluate peak-to-valley height, surface height distribution, and surface uniformity include the average and RMS roughness values. Qualitative and quantitative measurements of textural characteristics, such as surface irregularity, signs of porosity, and microstructural heterogeneity, were measured.

2.10. Electrical and dielectric properties

The electrical and dielectric behavior of the synthesized CMC was examined using a pellet-configured metal–insulator–metal device architecture. Squeezing the CMC powder led to the formation of a dense pellet 1.1 mm thick, and coating silver paste on both sides yielded reliable contacts. The effective electrode area obtained was 0.15 cm^2. Using a Keysight B290A source measure unit and a ZM2367 impedance analyzer, current–voltage (I—V) characteristics and AC impedance measurements were performed at room temperature to investigate the electrical conduction and dielectric behavior of the material. The dielectric loss behavior of a 1.1 mm thick CMC film was studied in terms of variation of conductance (G) with frequency. The complex dielectric constant characterizes the material's dielectric behavior as a function of frequency.

$$\varepsilon(\omega) = \varepsilon^{\prime}(\omega) - j\varepsilon^{\prime\prime}(\omega) \quad (8)$$

where $\varepsilon'(\omega)$is the real part of the dielectric constant (relative permittivity), whereas $\varepsilon''(\omega)$ is the imaginary component, representing dielectric loss and measuring the energy dissipated within the film. The real part of the dielectric constant was calculated using:

$$\varepsilon' = \frac{Ct}{\varepsilon_0 A} \quad (9)$$

where C is the measured capacitance, t is the dielectric thickness, A is the effective electrode area, and ε_0 is the permittivity of free space ($8.85 \times 10^{-12} F\, m^{-1}$).

The real part of the ε', also reduced as the frequency increased, in line with the common dielectric dispersion behavior observed in polymer-based materials. At a frequency of 1 MHz, the dielectric constant was measured to be 2.34, suggesting that electronic polarization is the primary mechanism at high frequencies. The dielectric constant (ε' ≈ 2.34 at 1 MHz) is comparable to reported values for cellulose-based dielectrics (ε' ≈ 2–5) [25,26], though lower than conventional high-k polymer dielectrics such as PVDF (ε' ≈ 8–12) [27,28].

The following relation was used to evaluate the imaginary part of the dielectric constant from conductance measurements:

$$\varepsilon'' = \frac{Gt}{\varepsilon_0 A\omega} \quad (10)$$

where $G = 1/R$ is the conductance and $\omega = 2\pi f$is the angular frequency.

The imaginary part, ε'', which indicates dielectric loss, was found to be 2 at 1 MHz, indicating energy dissipation owing to mechanisms such as charge carrier hopping and localized relaxation processes [29].

The dielectric loss tangent was calculated using

$$\tan(\delta) = \frac{\varepsilon''}{\varepsilon'} = \frac{G}{\omega C} \quad (11)$$

3. Results and discussion

3.1. Physical and chemical analyses

The CMC yield was found to be 70.3 ± 1.8%. This indicates that the extraction, alkalization of the cellulose, and etherification were performed efficiently with minimum material loss. The obtained CMC powder was found to have a density of 0.48 ± 0.03 g/cm^3. This shows that the powder has a porous and less tightly packed structure. This is good for dispersibility and hydration. The moisture content was established as 7.6 ± 0.4%, which is within acceptable levels for cellulose derivatives and allows proper stability during storage without being too hygroscopic. The aqueous solution (1%/vol) of CMC had a near-neutral pH of 7.1 ± 0.2, which proved that it neutralized the remaining alkali and showed the chemical purity of the product synthesized. The CMC was fully soluble in distilled water and formed a transparent homogeneous solution, which is due to the effective replacement of hydroxyl groups with hydrophilic carboxymethyl groups. The chemical analysis indicated a carboxyl content of 21.8 ± 0.9% or a degree of substitution value of 0.78 ± 0.04, which is within the reported optimal carboxyl content in industrial and commercial CMC [30]. All these findings corroborate the fact that *B. flabellifer* flower agro-waste is a potential and sustainable source of cellulose that can be used in the production of high-quality CMC for material, packaging, and other functional applications. Table 1 indicates that the physicochemical characteristics of CMC obtained using *B. flabellifer* flower agro-waste are very similar to those found in elucidated lignocellulosic materials such as sugarcane bagasse, rice straw, and banana pseudo-stem. The observed yield (70.3%) and density (0.48 g/cm^3) are within the range of agro-waste-based CMC, which demonstrates the effective etherification process and good powder properties. Equally, the moisture level (7.6), the near-neutral pH (7.1), and the carboxyl matter (21.8%) are all close to commercial-grade CMC values, and this confirms good chemical stability and purity. Notably, the level of substitution (0.78) falls within the optimum functional level, and it shows that *B. flabellifer* flower waste is a competitive and sustainable alternative cellulose source for CMC production.

3.2. FTIR analysis

The infrared (IR) spectra of the raw palm flower biomass, alkali-treated fiber, bleached cellulose, and synthesized CMC were obtained using FTIR to observe the structural changes that occurred during each stage, as illustrated in Fig. 2. Evidently, the spectral variations make it clear that the non-cellulosic components have progressively been removed and successfully carboxymethyl functional groups incorporated. The raw biomass spectrum shows a wide absorption band at about 3300–3400 cm^{-1}, corresponding to the O—H stretching vibration connected to cellulose, hemicellulose, and lignin. The peak around 2900 cm^{-1} is assigned to C—H stretching of aliphatic groups. A peak at 1730 cm^{-1} corresponds to C═O stretching of ester links in hemicellulose. Moreover, the peaks in the region of 1500–1600 cm^{-1} are assigned to the aromatic skeletal vibrations of lignin, thus confirming its lignocellulosic raw material [41]. After alkali treatment, there is a significant change in FTIR. The absence or decrease of the peak around 1730 cm^{-1} indicates effective hemicellulose removal. It suggests that partial delignification occurs because of their reduced intensity. Owing to the destructive impact of surrounding matrix components, exposure of hydroxyl moieties of cellulosic materials and broadening of the O—H stretching band takes place [42]. The whitened sample shows indications of extra purification. Almost total disappearance of peaks associated with lignin confirms that residual lignin was efficiently removed. The O—H stretching band stays intact whereas the peak around 1030–1060 cm^{-1} related to the C–O–C stretching vibrations of the cellulose backbone becomes stronger. This shows a relatively pure cellulose with improved structural regularity [43]. The FTIR spectrum of the synthesized CMC revealed distinct new absorption bands showing success in chemical modification. Peaks were obtained at the regions of 1580–1610 and 1410–1450 cm^{-1}, which correspond to the asymmetric and symmetric stretching vibrations of carboxylate (–COO−) groups, respectively. These peaks were not observed in the untreated and intermediate samples. The presence of the broad O—H band at 3300 cm^{-1} indicates that modification does not affect the cellulose backbone [44]. Overall, the FTIR data demonstrated that carboxymethyl groups were present in the cellulose and that lignin and hemicellulose were effectively removed during pretreatment. The material's hydrophilicity and dielectric qualities are improved by the addition of polar groups (–COO$^-$ groups). As a result, the produced CMC is a novel, environmentally feasible and sustainable material for electronic devices (Table 2).

3.3. XRD analysis

The XRD of raw, alkali, bleach, and CMC of the agro-waste of the *B. flabellifer* flower has a semi-crystalline structure of chemically substituted cellulose (Fig. 3). The raw biomass shows a broad diffraction peak at 2θ ≈ 22°, which is assigned to the (002) plane of cellulose I, and a slight hump at ~15–16° may be due to amorphous components, lignin and hemicellulose. The alkali treatment of the fiber increases the intensity of the peak at 2θ = 22° and sharpens it slightly. This indicates the partial removal of hemicellulose and lignin, which form an amorphous structure. This leads to better arrangement of cellulose chains and a corresponding increase in crystallinity. The bleached sample has been found to have an enhanced and sharper peak at 2θ = 22° along with a decreased amorphous halo. This means the residual lignin and hemicellulose have been removed effectively, resulting in high-purity cellulose with improved crystallinity. The CMC sample exhibits a significant change in the diffraction pattern. New peaks or noise in the 30–40° range become more noticeable, while the usual cellulose peak at about 22° broadens and diminishes. This implies that the crystalline structure

Table 1
Physicochemical property analysis of some CMC bio resources.

Sl. No.	Cellulose Source	Yield (%)	Bulk Density (g cm^{-3})	Moisture (%)	pH (1% soln)	Carboxyl Content (%)	DS	Reference
1	Sugarcane bagasse	72.5	0.46	7.2	7.0	22.1	0.82	[31]
2	Banana pseudostem	68.9	0.44	8.1	6.9	20.6	0.76	[32]
3	Rice straw	70.1	0.49	7.8	7.2	21.4	0.79	[33]
4	Oil palm Empty fruit bunch	73.4	0.51	6.9	7.3	22.8	0.85	[34]
5	Water hyacinth (*Eichhornia crassipes*)	66.8	0.43	8.6	6.8	19.9	0.72	[35]
6	Corncob residue	69.7	0.47	7.5	7.1	21.0	0.78	[36]
7	Cotton linter waste	75.2	0.52	6.4	7.4	24.1	0.92	[37]
8	Bamboo fiber	71.6	0.48	7.9	7.2	20.8	0.74	[38]
9	Cassava peel	67.4	0.45	8.3	6.9	20.1	0.75	[39]
10	Hardwood pulp	74.0	0.50	6.7	7.3	23.2	0.88	[40]
11	*B. flabellifer* flower	70.3	0.48	7.6	7.1	21.8	0.78	This study

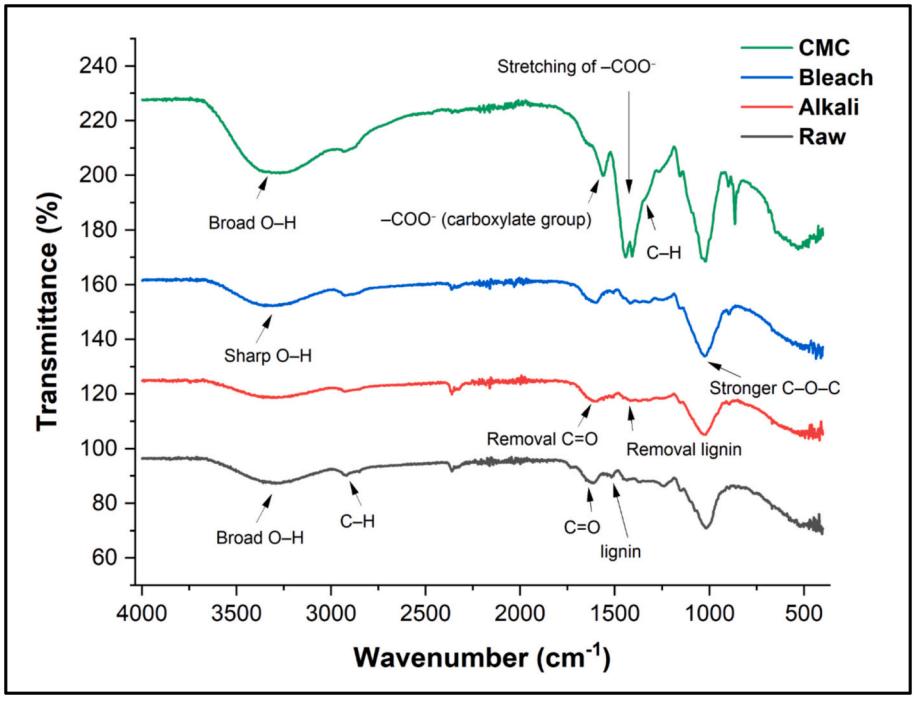

Fig. 2. FTIR analysis of raw, alkali, bleach, and CMC from *B. flabellifer* flower waste.

Table 2
FTIR peak arrangement table of CMC from *B. flabellifer* waste.

Sl. No	Peak Range (cm^{-1})	Observed Peak (cm^{-1})	Functional Group Assignment
1	3200–3600	~3330	O–H stretching (hydrogen-bonded hydroxyl groups)
2	2800–3000	~2900	C–H stretching (aliphatic –CH, $–CH_2$ groups)
3	1580–1610	~1600	Asymmetric stretching of $–COO^-$ (carboxylate group)
4	1400–1450	~1420	Symmetric stretching of $–COO^-$
5	1320–1360	~1330	O–H bending / C—H deformation
6	1200–1270	~1230	C–O stretching (ether linkage)
7	1000–1100	~1050	C–O–C stretching (cellulose backbone)
8	890–950	~900	β-Glycosidic linkage (C—H rocking)
9	700–800	~750	CH_2 rocking/skeletal vibrations

of cellulose is disturbed by the addition of carboxymethyl groups (CH_2COO^-). Cellulose's organized structure is changed into the more amorphous polymer characteristic of CMC through the substitution process.

Peak deconvolution of the experimental pattern into individual crystalline contributions and an amorphous background shows a significant decrease in crystalline order compared to that of native cellulose, which is anticipated following carboxymethylation because intermolecular hydrogen bonding is disturbed. The computed CI (Eq. 5) of the crystalline and amorphous areas of the deconvoluted peaks was determined to be 48.6%, implying a partial loss of crystallinity, which was experienced due to the alkalization and purification of crystalline hydroxyl groups with the carboxyl substituents. Such a CI value is in the normal range of biomass-produced CMC (35–60) and is an indication of effective chemical modification without cellulose backbone destruction. The mean CS determined (Eq. 6) as the FWHM of the primary crystalline peak by the Scherrer method was obtained as 4.2 nm on average. The crystallite size indicates that the nanoscale is an indication that the regenerated cellulose crystallites may undergo fragmentation into a smaller ordered domain during alkalization treatment and carboxymethylation. These diminished crystallite sizes have the benefit of improved solubility, swelling characteristics, and interfaces that are essential to sustainable material and biopolymer operations. In general, the XRD findings support the conversion of the native cellulose to semi-crystalline CMC, with lower crystallinity in addition to nanoscale crystallite size similar to those of CMC prepared using other agro-wastes of lignocellulosic materials, as summarized in Table 3. *B. flabellifer* CMC was crystallized moderately (CI 48.6% CS 4.2 nm) relative to pineapple leaf (~49.85%) and commercial CMC (~52.03%). The drop in crystallinity of CMC is good for its dielectric application as the presence of a greater amorphous region improves dipolar mobility and ionic conduction, and thereby dielectric property.

3.4. SEM analysis

The SEM results of *B. flaberllifer* flower waste CMC are shown in Fig. 4[a–f]. Figs. 4[a] and 4[b] show the CMC had acicular fibrous and clustered structures, which are indicative of the development of elongated crystalline fibrils with interlaced networks, which is characteristic of cellulose derivatives. The fibrillar structure indicates that the structure is easily changed in the carboxymethylation process to produce an increase in surface area and possible water contact. During intermediate magnifications (×1000, Fig. 4[c]), the microstructure showed heterogeneous acicular-flaky structures, which suggest that the fibers were partly combined in lamellar-like structures. This morphology suggests that it retains reticulose fibrous cellulose structures in addition to showing flake formation as a result of modification. At reduced magnifications (Figs. 4[d–f]), non-uniform lamellar structures, rough scattered grains, and particulate-fibrous structures were revealed, which depict the switch between micro-fibrils and more compact aggregates. The crude and porous characteristic of these particles implies that they are highly substituted and porous, which may be more useful in water retention, swelling, and functional activity when it comes to sustainable use of material. Thus, the SEM analysis confirms the *B. flabellifer* CMC has a multiscale morphology that morphologically combines fibrous, flaky, and particulate structures, which are advantageous to its application in biodegradable composites and other environmentally friendly materials [52]. SEM research on the CMC of *B. flabellifer* flower also

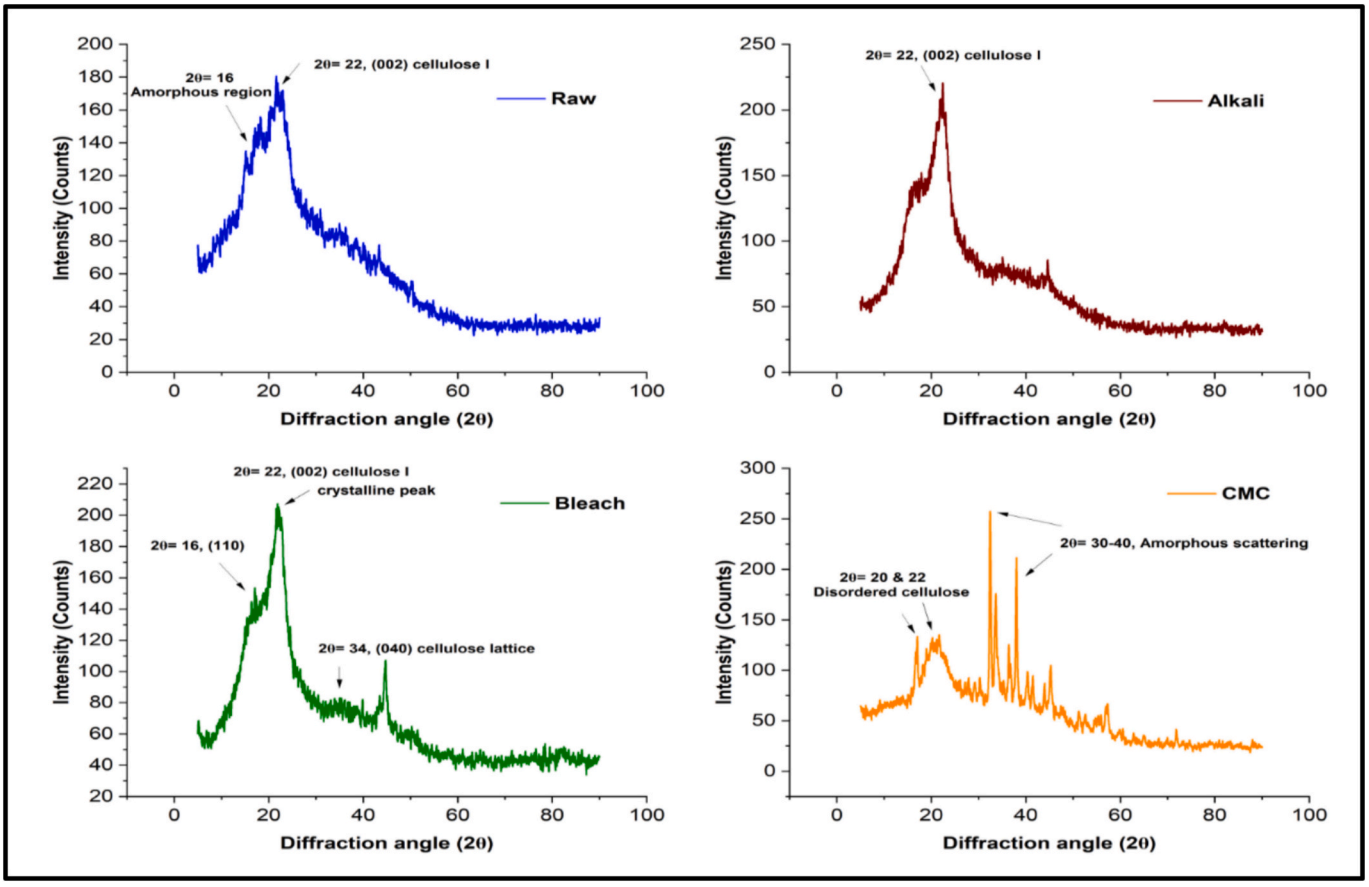

Fig. 3. X-ray diffraction analysis of CMC from *B. flabellifer* flower waste.

Table 3
Crystallinity properties of some CMC resources.

Sl. No.	Material/Source	CI (%)	CS (nm)	Reference (with DOI/ Link)
1	As-synthesized CMC (pineapple leaf)	~49.85	–	[40]
2	Commercial CMC	~52.03	–	[45]
3	CMC–CNC nanocomposite	44.8	5.20	[46]
5	Pure CNC (control)	73.3	4.02	[47]
6	CMC with graphene nanofiller	–	40.92–80.71	[48]
7	α-Cellulose (precursor)	67.62	–	[49]
8	CMC-SCL (NaOH treated)	43.37–50.50	–	[50]
9	Alkali-cellulose (intermediate)	69.16	–	[51]
10	*B. flabellifer* CMC	48.6	4.2	Present work

finds that the CMC of cassava peel has a multiscale structure with preferred tenuous or irregular surface morphology, which is probably attributed to extensive amorphization of the material after carboxymethyl extraction [53]. The distinct structure is possibly an inherent hierarchy of the original cellulose fibers, as well as a combination of the extraction and carboxymethylation conditions, implying an improved surface area, porosity, and functionality toward sustainable material use.

3.5. EDS analysis

Elemental analysis of the CMC extracted from the flowers of *B. flabellifer* was analyzed using EDS, as shown in Fig. 5[a–c]. The spectrum indicated the presence of carbon (C), oxygen (O), sodium (Na), and chlorine (Cl), which have mass percentages of 28.63, 33.32, 24.51, and 13.55, respectively. Both the presence of high carbon and oxygen content are in line with the polysaccharide backbone of the cellulose structure, proving that the cellulose structure is still intact after carboxymethylation.

The large quantities of sodium imply the successful addition of carboxymethyl groups to create the sodium salt of CMC, and the chlorine found is probably due to remaining NaCl from the neutralization process of the synthesis. These homogeneous values of the elements, given by the similarity in the values of the cellulose fibers at the spot being analyzed, show a uniform alteration in the cellulose fibers [54]. Thus, the EDS investigations reveal the successful functionalization of *B. flabellifer* cellulose into CMC, with the elemental composition indicating its possible hydrophilicity, improved water absorption, and ability to be used in the creation of sustainable biopolymer material.

3.6. Particle size analysis

The particle size analysis is shown in Fig. 6 [a–d]. The SEM micrographs, examined under ×250 magnification, which show irregularly shaped and angular particles with rough surfaces and no harsh agglomeration, which means that the processing has achieved size reduction. The image measurements indicate a projected area of the particles to be in the range of 10^{-4} mm^2 which is a micro-sized particulate system. The measured particles were statistically assessed, showing that the mean size of the particles was 0.067 mm, and the

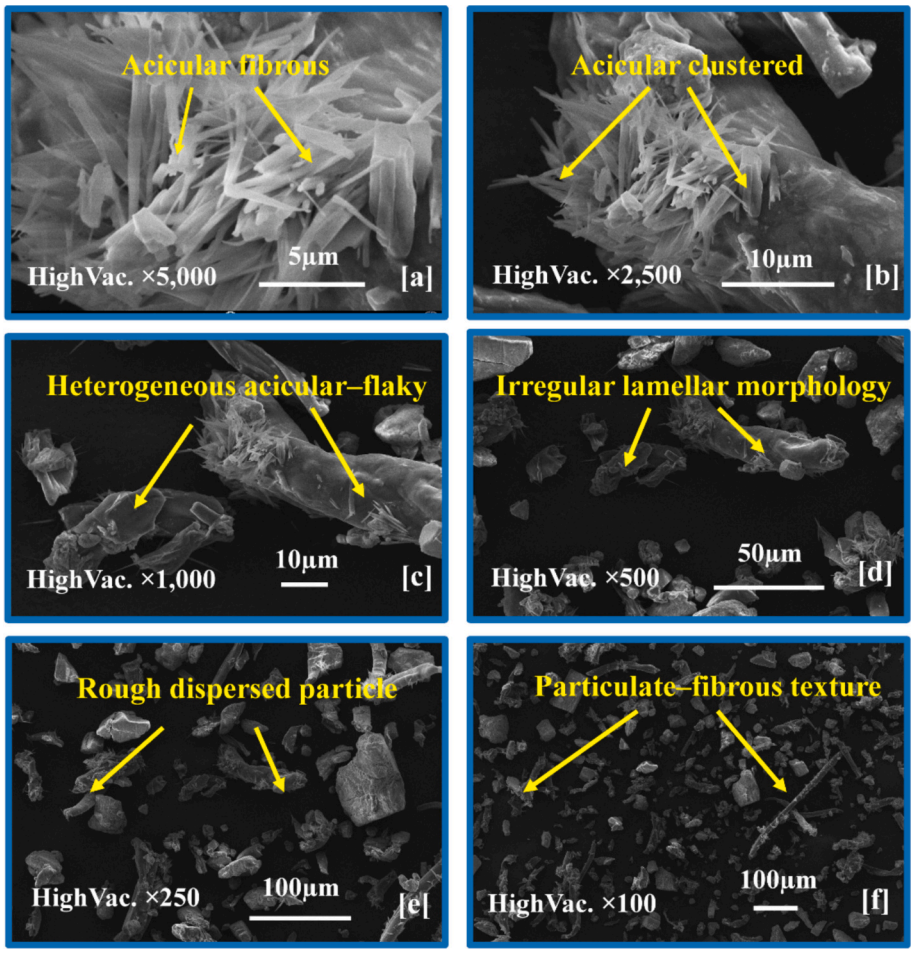

Fig. 4. SEM analysis of CMC from *B. flabellifer* flower waste.

standard deviation was 0.027 mm, which is observed to be moderately spread around the average. The histogram of the particle size distribution has an approximately normal (Gaussian) trend, indicating that the size distribution of the particles is not bimodal or highly skewed but is uniformly distributed. The coarse and fine fractions were found to coexist with minimum and maximum particle sizes of about 0.029 and 0.112 mm, respectively. This type of distribution is beneficial as smaller particles will add to the surface area and reactivity, whereas larger particles will assist in packing efficiency and mechanical stability. Finally, the particle size analysis shows that the size reduction is controlled and that the uniformity is acceptable, which means that the material can be used in composite reinforcement, film formation, and other functional material systems when a balance of surface area and structural integrity is needed.

3.7. Surface roughness analysis

The AFM topographical analysis (Fig. 7) was used to measure the surface roughness properties of the synthesized material on a quantitative basis to give information on surface morphology, height distribution, and texture uniformity. The AFM images in Fig. 7[A–E] indicate that the surface is highly irregular and heterogeneous with sharp peaks and valleys, which indicate that the cellulose structure was effectively modified and disrupted with fibrils. The measured values for the arithmetic mean roughness (R_a) and root mean square roughness (R_q) were 35.90 and 42.75 nm, respectively, which proved a moderately rough surface with great height variations. The negative value of skewness ($R_{sk} = -0.106$) indicates the presence of more valleys than sharp protrusions, whereas the positive value of kurtosis ($R_{ku} = 0.602$) represents a relatively wide range of heights without any extreme spikes, which is indicative of homogeneous surface evolution throughout the processing process. The overall height of the surface profile (R_t) was 234.42 nm, the peak of profile height (R_p) was 173.12 nm, and the valley depth maximum (R_v) was −61.30 nm, which shows that well-formed surface asperities are present. These findings are further supported by three-dimensional surface mapping, which indicates that there are closely spaced ridges and depressions that increase the surface area. This greater surface roughness has the benefit of enhancing the level of interaction between surfaces, in the sense that it can enhance wettability, adhesion, and compatibility in composite matrices, film formation, and coating. Altogether, the AFM roughness parameters testify to the fact that the synthesized material in question has a structurally active and topographically complex surface that can be used in advanced material and functional applications.

3.8. Electrical and dielectric properties

The *I*—*V* characteristics of the CMC pellet were recorded under an applied bias voltage, as shown in Fig. 8. The sample showed minimal leakage current over the entire applied voltage range, indicating its insulating behavior. The current reached a value of approximately 8.1 μA when a bias voltage of 20 V was applied. The steady increase in current with applied voltage implies that charge transport is likely governed by a bulk-controlled conduction mechanism, most probably due to thermally activated carrier hopping and minor ionic displacement in the polymer [55]. The registered current is relatively low due to the good dielectric strength of the pellet, which determines its use in dielectric and insulating applications in electronic devices.

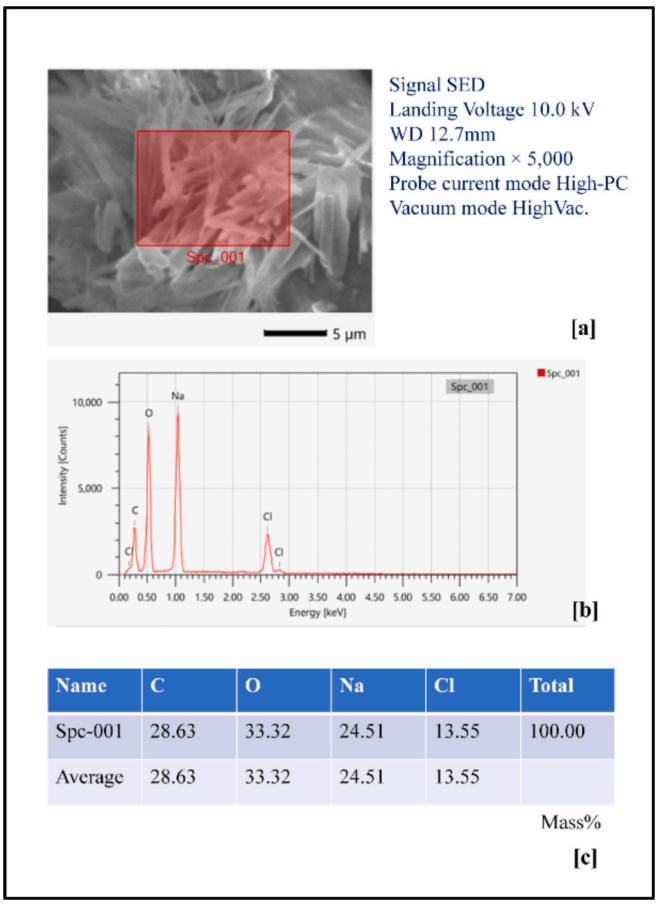

Name	C	O	Na	Cl	Total
Spc-001	28.63	33.32	24.51	13.55	100.00
Average	28.63	33.32	24.51	13.55	

Mass%

[c]

Fig. 5. EDS analysis [a] area of selection, [b] peak analysis, [c] data of CMC from *B. flabellifer* flower waste.

Impedance spectroscopy study was performed in the frequency range of 2 kHz to 1 MHz, and the measured response has been fitted in terms of the parallel resistance (R_p), parallel capacitance (C_p), and dissipation factor (D).

In the model, the parallel resistance (R_p) refers to the bulk resistance responsible for charge transport and leakage processes, whereas the parallel capacitance (C_p) refers to the capacitive contribution from polarization processes in the CMC matrix. As frequency increases, R_p reduces, indicating that higher frequency charge carrier mobility is enhanced and relaxation is faster, as shown in Fig. 9[a]. At low frequencies, high R_p values are attributed to limited charge transport due to electrode polarization effects and restricted carrier hopping. The value of R_p was reduced to approximately 6.38 MΩ at 1 MHz, which shows low impedance toward AC excitation. This behavior depends on frequency and is mostly seen in a polar polymer dielectric showing space-charge and interfacial polarizations [56].

Fig. 9[b] reveals that as frequency increased, there is a gradual decrease in C_p with the increase of frequency. At lower frequencies, due to the slow variations of the electric field, there is an important contribution of the dipolar, interfacial, and ionic polarization mechanisms to capacitance. With an increase in frequency, the slower polarization mechanisms cannot keep up with the rapidly reversing electric field. Therefore, C_p decreases. At the highest measured frequency of 1 MHz, the value of C_p reached 0.28 pF, suggesting that slower processes such as interfacial and dipolar polarization made little lasting contribution, and electronic polarization is the main process [57]. The dielectric constant (ε') gradually decreases as the frequency increases and reaches a value of 2.34 at 1 MHz. This value lies within the typical range reported for cellulose-based dielectrics and indicates a moderate level of polarization in the material. The CMC dielectric constant (ε' ≈ 2.34 at 1 MHz) is similar to values reported for cellulose-based dielectrics (ε' ≈ 2–5), but lower than high-k polymers such as PVDF. However, the loss tangent is significantly higher than conventional insulating polymers, indicating greater dielectric dissipation.

At 1 MHz, the loss tangent was calculated as 0.87, indicating progressively moderate dielectric loss with an increase in frequency, as

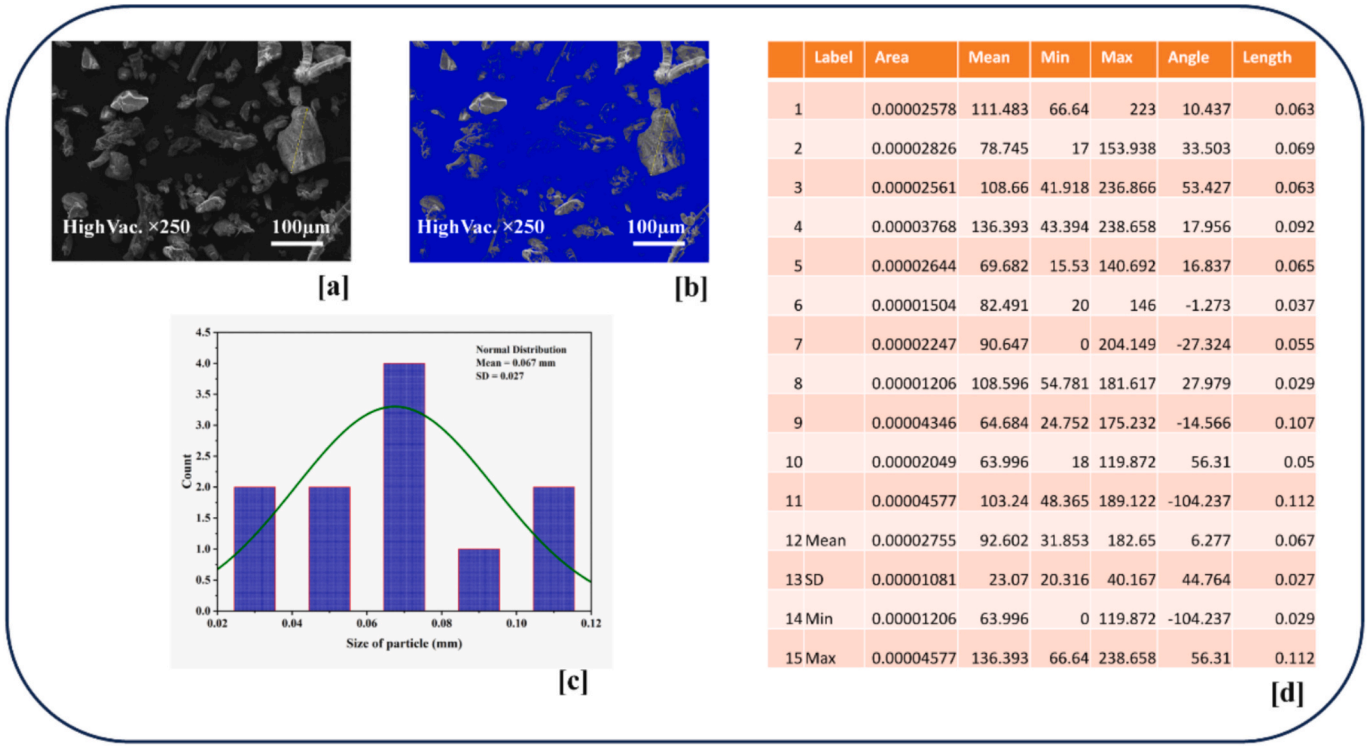

	Label	Area	Mean	Min	Max	Angle	Length
1		0.00002578	111.483	66.64	223	10.437	0.063
2		0.00002826	78.745	17	153.938	33.503	0.069
3		0.00002561	108.66	41.918	236.866	53.427	0.063
4		0.00003768	136.393	43.394	238.658	17.956	0.092
5		0.00002644	69.682	15.53	140.692	16.837	0.065
6		0.00001504	82.491	20	146	-1.273	0.037
7		0.00002247	90.647	0	204.149	-27.324	0.055
8		0.00001206	108.596	54.781	181.617	27.979	0.029
9		0.00004346	64.684	24.752	175.232	-14.566	0.107
10		0.00002049	63.996	18	119.872	56.31	0.05
11		0.00004577	103.24	48.365	189.122	-104.237	0.112
12	Mean	0.00002755	92.602	31.853	182.65	6.277	0.067
13	SD	0.00001081	23.07	20.316	40.167	44.764	0.027
14	Min	0.00001206	63.996	0	119.872	-104.237	0.029
15	Max	0.00004577	136.393	66.64	238.658	56.31	0.112

[d]

Fig. 6. Particle size analysis: [a] SEM image, [b] threshold area, [c] histogram, [d] data of CMC from *B. flabellifer* flower waste.

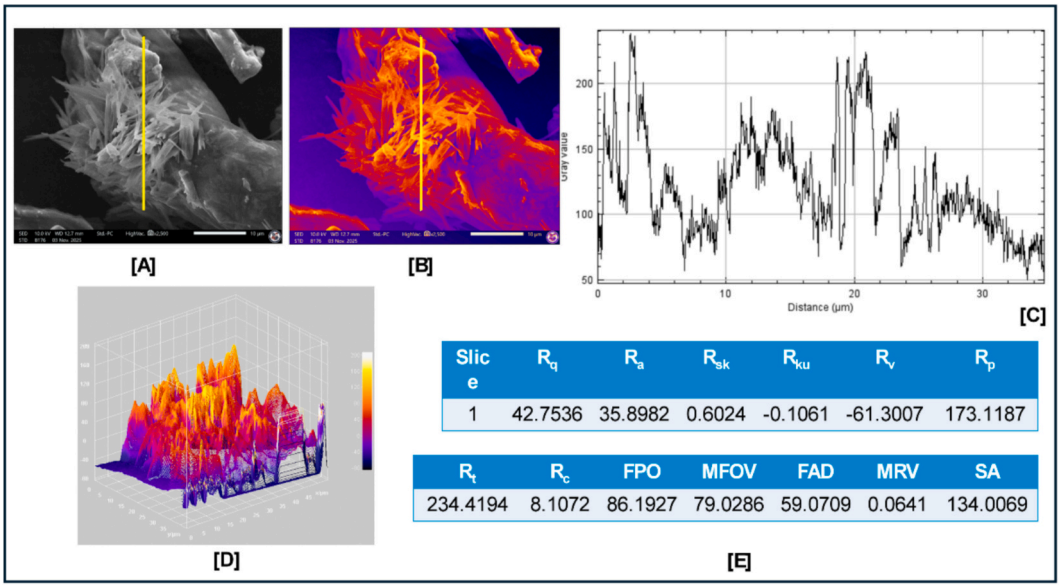

Slice	R_q	R_a	R_{sk}	R_{ku}	R_v	R_p
1	42.7536	35.8982	0.6024	-0.1061	-61.3007	173.1187

R_t	R_c	FPO	MFOV	FAD	MRV	SA
234.4194	8.1072	86.1927	79.0286	59.0709	0.0641	134.0069

Fig. 7. Surface roughness analysis: [a] vertical line plot, [b] threshold image, [c] plot profile graph, [d] 3D surface plot, and [e] roughness parameters of CMC from *B. flabellifer* flower waste.

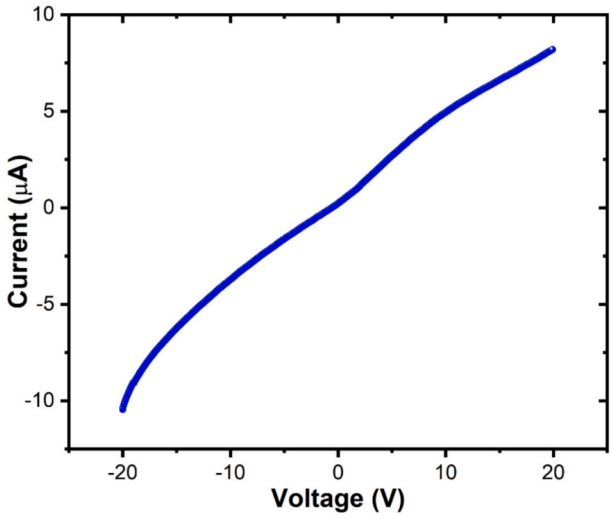

Fig. 8. Determination of current–voltage (*I*—*V*) properties of the CMC pellet at room temperature.

ionic and dipolar polarization contributions start to fall off, as shown in Fig. 10. This phenomenon occurs because the slower polarization processes, such as dipolar and ionic polarization, cannot follow the rapidly fluctuating electric field, which consequently leads to high dielectric losses at higher frequencies. The noted frequency-dependent dielectric dispersion and high loss tangent obtained from Eqs. 8–11 are linked to the increase in amorphous fraction in CMC, which favors ionic displacement and dipolar mobility. Significant ionic and dipolar loss contributions are indicated by the observed loss tangent (tanδ ≈ 0.87 at 1 MHz), which is higher than that of commercial insulating polymers (usually <0.1). The relatively high loss tangent observed at higher frequencies shows significant dielectric loss, which limits the suitability of the material for high-performance capacitor applications. The presence of polar functional groups (–OH, $–COO^-$) and residual ionic species in CMC is responsible for its relatively high loss tangent. Ion migration and interfacial polarization mechanisms of these groups promote polarization while enhancing dielectric loss. The dielectric response of the CMC pellet can be interpreted using the Maxwell–Wagner–Sillars interfacial

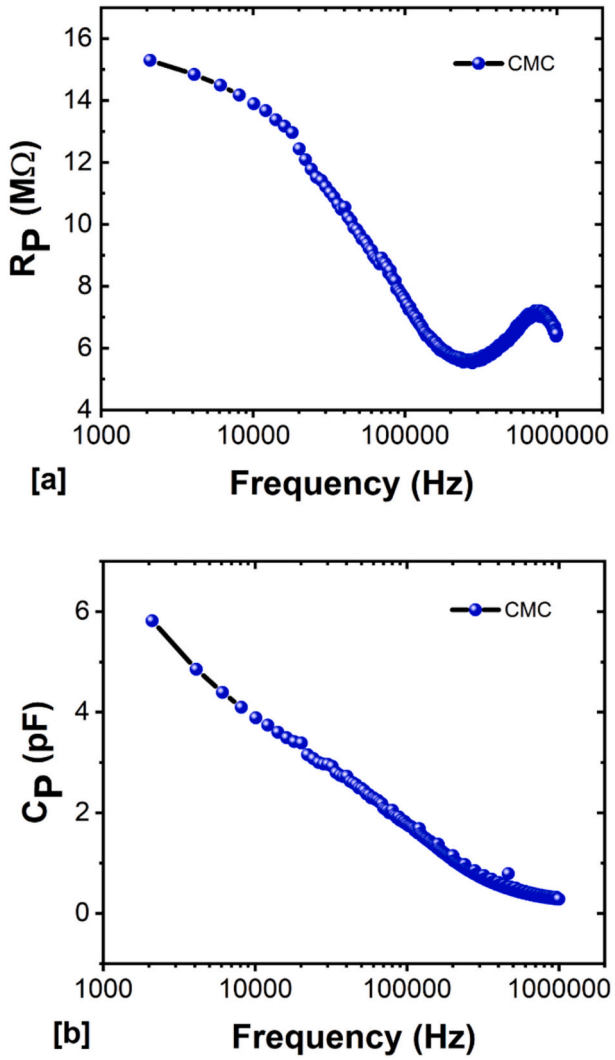

Fig. 9. [a] Frequency dependence of parallel resistance (R_p), and [b] variation of parallel capacitance (C_p) as a function of frequency for the CMC pellet.

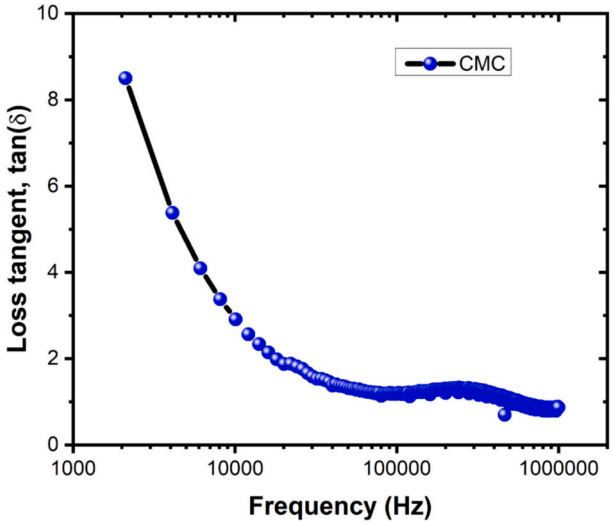

Fig. 10. Variation of loss tangent (tan δ) with frequency for the CMC pellet, suggesting reduced dielectric loss at higher frequencies.

polarization framework, which accounts for charge piling up at the interfaces of charge transport [58]. At low frequencies, the most significant factors are space charge and dipolar polarization. This results in an increase in dielectric constant and losses. With increasing frequency, these slower polarization mechanisms are rendered ineffective in keeping pace with the applied field, which results in reduced ε' and tanδ.

According to the DC and AC electrical measurements, CMC has low leakage current, high bulk resistance, a dielectric constant which varies with frequency, and well-regulated dielectric loss, a characteristic of a moderate dielectric material with notable loss characteristics. The observed dielectric dispersion corresponds with the polyelectrolyte characteristics of CMC, where at lower frequencies, the contribution from mobile ions and dipolar functional groups is major. The findings confirm the dielectric properties of cellulose-based materials obtained in the literature and suggest CMC is a sustainable dielectric material. The authors report that CMC can be used in low-power, biodegradable, and environmentally friendly electronic applications, but not in high-performance electronic devices [59]. The dielectric properties of the synthesized CMC are strongly influenced by its structural characteristics. As indicated by the degree of substitution (DS = 0.78) obtained, carboxymethyl groups were successfully incorporated into the cellulose backbone, disrupting the hydrogen bonding network of native cellulose. This change causes a certain decrease in crystallinity, increasing the amount of amorphous area in the structure of the polymer, according to the XRD study. Furthermore, the SEM images display a porous and rough structure that can inspire charge transfer and dipolar polarization in the event of an electric field. The structural changes taken together influence the electrical response of the material, such as measured leakage current and dielectric loss. A comparison with reported dielectric materials indicates that the dielectric constant of the present CMC falls within the typical range for cellulose-based systems (ε' ≈ 2–5). Despite demonstrating dielectric behavior, the relatively high loss tangent (tan δ ≈ 0.87 at 1 MHz) indicates considerable energy dissipation within the material. This value is significantly higher than that of conventional dielectric polymers, which typically exhibit tan δ values below 0.1. In contrast to frequently used dielectric materials, such as polyethylene and PVDF, which have much lower dielectric loss (0.001–0.05), the higher dielectric loss observed in this study is due to the presence of polar groups and residual ions in the CMC [60]. Even compared to bio-derived dielectric films such as cellulose and starch films, which typically have tan δ between 0.01and 0.2, the current material has significantly higher energy loss [61]. This increases dipolar polarization but also leads to loss, which restricts its application in high-frequency and high-energy devices. In modern society, inductive charging for the infrastructure applications' potential is also possible. This study supports dual functionality in civil and electronic appliances.

4. Conclusions

This study assessed the potential and underutilized lignocellulosic biomass of *B. flabellifer* flower agro-waste for the extraction of CMC. The alkalization, bleaching, and purification process that was developed gave CMC a 70.3% yield, a neutral pH (7.04), and complete dissolution in water, which confirmed the suitability of the modification process. The degree of substitution of CMC was 0.79, and the carboxyl content was 21.8%, which confirmed the introduction of the carboxyl groups in the cellulose backbone. FTIR and XRD characterizations of the structure show the existence of carboxylate functionalities and a drop in the crystal structure (48.6%), showing more amorphous sites that will help in water uptake and interfacial forces. A morphological study showed that the different fibers and particles are heterogeneous and have average surface rugae, which leads to better compatibility in composites and film-forming. The leakage current of CMC pellets was reported to be 8.1 μA at 20 *V*, with the loss tangent range reported to be 0.87. Dielectric behavior was reported to be average and also dependent on the polar functional groups and structural changes of the cellulose structure. Thus, the prepared CMC exhibits a moderate dielectric response and can be used as a sustainable and renewable material for low-power electronics. This research is mainly aimed at demonstrating the potential of using *B. flabellifer* flower agro-waste as a bio-based dielectric material for electronic devices and also serving as a basis for future research in the future smart infrastructure applications with green electronic technology.

CRediT authorship contribution statement

Sunarkani Ganesh: Writing – review & editing, Writing – original draft, Conceptualization. **K. Vijaya Bhaskar Reddy:** Investigation, Formal analysis. **K. Chaithanya:** Visualization, Supervision. **Sagar Dnyandev Patil:** Methodology, Investigation. **T. Senthil Vadivel:** Formal analysis, Data curation, Conceptualization. **R. Mallikarjun:** Visualization, Methodology. **Sunesh Narayanaperumal:** Writing – review & editing, Writing – original draft, Conceptualization. **Indran Suyambulingam:** Supervision, Investigation. **Sivarao Subramonian:** Validation, Supervision. **Siva Avudaiappan:** Formal analysis.

Consent to participate

Not applicable.

Consent to publish

Not applicable.

Ethical approval

Not applicable.

Funding

The authors declare no funds available for this manuscript.

Declaration of competing interest

The authors declare that they have no known competing financial interests or personal relationships that could have appeared to influence the work reported in this paper.

Acknowledgements

The authors extend their thanks to the Department of Mechanical Engineering, Marri Laxman Reddy Institute of Technology and Management, for supporting this research work.

Data availability

Data will be made available on request.

References

[1] J. Wei, S. Jia, L. Zhang, Y. Zhou, Y. Lv, X. Zhang, Z. Shao, Preparation of treelike and rodlike carboxymethylated nanocellulose and their effect on carboxymethyl cellulose films, J. Appl. Polym. Sci. 138 (2021), https://doi.org/10.1002/app.50092.

[2] D.M. dos Santos, A. de L. Bukzem, D.P.R. Ascheri, R. Signini, G.L.B. de Aquino, Microwave-assisted carboxymethylation of cellulose extracted from brewer's spent grain, Carbohydr. Polym. 131 (2015) 125–133, https://doi.org/10.1016/j.carbpol.2015.05.051.

[3] Z. Kassab, E. Syafri, Y. Tamraoui, H. Hannache, A.E.K. Qaiss, M. El Achaby, Characteristics of sulfated and carboxylated cellulose nanocrystals extracted from Juncus plant stems, Int. J. Biol. Macromol. 154 (2020) 1419–1425, https://doi.org/10.1016/j.ijbiomac.2019.11.023.

[4] C. Liu, H. Wang, M. Usman, M. Ji, J. Sha, Z. Liang, L. Zhu, L. Zhou, B. Yan, Nonmonotonic effect of CuO nanoparticles on medium-chain carboxylates production from waste activated sludge, Water Res. 230 (2023) 119545, https://doi.org/10.1016/j.watres.2022.119545.

[5] A. Dzigbor, D. Neglo, C.S. Dzah, R. Sraha, Total phenolic content, phytochemical screening, antioxidant and antimicrobial activities of Borassus flabellifer and Borassus aethiopum fruits, Food Chemistry Advances 7 (2025) 100937, https://doi.org/10.1016/j.focha.2025.100937.

[6] K. Obi Reddy, C. Uma Maheswari, M. Shukla, J.I. Song, A. Varada Rajulu, Tensile and structural characterization of alkali treated Borassus fruit fine fibers, Compos. Part B Eng. 44 (2013) 433–438, https://doi.org/10.1016/j.compositesb.2012.04.075.

[7] S. Dubey, A. Shukla, R.K. Shukla, A. Kumar, Nutritional value, phytochemical content, and pharmacological screening of *Borassus flabellifer* L. fruits, Nat. Prod. Res. (2025) 1–8, https://doi.org/10.1080/14786419.2025.2453511.

[8] J.K. Singh, A.K. Rout, Characterization of raw and alkali-treated cellulosic fibers extracted from Borassus flabellifer L, Biomass Convers. Biorefinery 14 (2024) 11633–11646, https://doi.org/10.1007/s13399-022-03238-x.

[9] G.A. Sivasankar, C.B. Moorthy, S. Kaliappan, R. Sathyamurthy, T. Sathish, R. Saravanan, Ü. Ağbulut, Sustainable nano-added biofuel production from borassus flabellifer oil for conventional internal combustion engines, Energy 282 (2023) 128381, https://doi.org/10.1016/j.energy.2023.128381.

[10] A.S. Nizami, M. Rehan, M. Waqas, M. Naqvi, O.K.M. Ouda, K. Shahzad, R. Miandad, M.Z. Khan, M. Syamsiro, I.M.I. Ismail, D. Pant, Waste biorefineries: enabling circular economies in developing countries, Bioresour. Technol. 241 (2017) 1101–1117, https://doi.org/10.1016/j.biortech.2017.05.097.

[11] Md.S. Rahman, Md.S. Hasan, A.S. Nitai, S. Nam, A.K. Karmakar, Md.S. Ahsan, M.J. A. Shiddiky, M.B. Ahmed, Recent developments of Carboxymethyl cellulose, Polymers (Basel). 13 (2021) 1345, https://doi.org/10.3390/polym13081345.

[12] K. Lal, R.K. Yadav, R. Kaur, D.S. Bundela, M.I. Khan, M. Chaudhary, R.L. Meena, S. R. Dar, G. Singh, Productivity, essential oil yield, and heavy metal accumulation in lemon grass (Cymbopogon flexuosus) under varied wastewater–groundwater irrigation regimes, Ind. Crop. Prod. 45 (2013) 270–278, https://doi.org/10.1016/j.indcrop.2013.01.004.

[13] X. Wang, P. Wang, J. Ma, H. Liu, P. Ning, Synthesis, characterization, and reactivity of cellulose modified nano zero-valent iron for dye discoloration, Appl. Surf. Sci. 345 (2015) 57–66, https://doi.org/10.1016/j.apsusc.2015.03.131.

[14] E.H. Boutriouia, T. El Assimi, M. Raihane, R. Beniazza, H. Ben Youcef, M. Khouloud, M.H.V. Baouab, A. El Kadib, M. Lahcini, Polymethyl methacrylate-g-carboxy-methylcellulose as an amphiphilic coating material for slow-release fertilizer, Prog. Org. Coat. 172 (2022) 107102, https://doi.org/10.1016/j.porgcoat.2022.107102.

[15] V.S. Munagapati, H.-Y. Wen, J.-C. Wen, K.-Y.A. Lin, Y. Gutha, A.R.K. Gollakota, V. Yarramuthi, K. Rudravarapu, S. Sangaraju, H.Y. Choi, Biopolymer-inorganic hybrid composites: the expanding role of cellulose/layered double hydroxides (LDHs) in advanced applications, Inorg. Chem. Commun. 179 (2025) 114795, https://doi.org/10.1016/j.inoche.2025.114795.

[16] F. Khoshdouni Farahani, A.R. Oromiehi, A. Sharifan, Z. Khoshdouni Farahani, Edible films solution developed from carboxymethyl cellulose / sesame oil: physical, mechanical and microbial attributes of films, applied, Food Res. 5 (2025) 100771, https://doi.org/10.1016/j.afres.2025.100771.

[17] W. Wongvitvichot, S. Pithakratanayothin, S. Wongkasemjit, T. Chaisuwan, Fast and practical synthesis of carboxymethyl cellulose from office paper waste by ultrasonic-assisted technique at ambient temperature, Polym. Degrad. Stab. 184 (2021) 109473, https://doi.org/10.1016/j.polymdegradstab. 2020.109473.

[18] F.E. Okieimen, D.E. Ogbeifun, Graft copolymerizations of modified cellulose: grafting of methyl acrylate, ethyl acrylate and ethyl methacrylate on carboxy methyl cellulose, Eur. Polym. J. 32 (1996) 311–315, https://doi.org/10.1016/0014-3057(95)00152-2.

[19] J. Lei, L. Deng, Z. Chen, X. Li, K. Li, J.-M. Lee, Efficient in situ saccharification of microcrystalline cellulose over immobilized cellulase on magnetic biochar in ionic liquid media, Chem. Eng. J. 485 (2024) 149990, https://doi.org/10.1016/j.cej.2024.149990.

[20] P.S. Bednarek, P.B. Kowalczuk, Cellulose and its derivatives as a sustainable reagent in mineral flotation: mechanisms and applications, Sep. Purif. Technol. 378 (2025) 134690, https://doi.org/10.1016/j.seppur.2025.134690.

[21] H.M.S. Akhtar, S. Ahmed, E. Olewnik-Kruszkowska, M. Gierszewska, M. S. Brzezinska, K. Dembińska, A. Kalwasińska, Carboxymethyl cellulose based films enriched with polysaccharides from mulberry leaves (Morus alba L.) as new biodegradable packaging material, Int. J. Biol. Macromol. 253 (2023) 127633, https://doi.org/10.1016/j.ijbiomac.2023.127633.

[22] K. Bin Bandar, M.K. Aleid, S. Aljlil, L.A. Albedair, A.S. Al-Wasidi, A.A.H. Bukhari, R.A.S. Alatawi, I.S.S. Alatawi, J.S. Alnawmasi, N.H. Elsayed, Synthesis and characterization of magnetic aluminum metal-organic frameworks encapsulated with chitosan and carboxymethyl cellulose for effective elimination of atrazine from aqueous solutions: adsorption evaluation, DFT calculations and box-Behnken design optimization, Int. J. Biol. Macromol. 282 (2024) 137359, https://doi.org/10.1016/j.ijbiomac.2024.137359.

[23] F. Tang, C. Wang, L. Zhang, Z. He, F. Huang, Sustainable transformation of waste cotton into quaternized carboxy cellulose nanocrystals enables chain-enhanced adsorption for industrial textile wastewater purification, Carbohydr. Polym. 372 (2026) 124580, https://doi.org/10.1016/j.carbpol.2025.124580.

[24] B.B. Kassie, T.M. Daget, D.F. Tassew, Synthesis, functionalization, and commercial application of cellulose-based nanomaterials, Int. J. Biol. Macromol. 278 (2024) 134990, https://doi.org/10.1016/j.ijbiomac.2024.134990.

[25] A. Khouaja, A. Koubaa, H. Ben Daly, Study of the dielectric and chemical properties of cellulose bio-based composites, Ind. Crop. Prod. 214 (2024), https://doi.org/10.1016/j.indcrop.2024.118493.

[26] M. Lecoublet, M. Ragoubi, N. Leblanc, A. Koubaa, Sustainable 3D-printed cellulose-based biocomposites and bio-nano-composites: analysis of dielectric performances, Ind. Crop. Prod. 221 (2024), https://doi.org/10.1016/j.indcrop.2024.119332.

[27] L. Padurariu, E. Brunengo, G. Canu, L.P. Curecheriu, L. Conzatti, M.T. Busaglia, P. Stagnaro, L. Mitoseriu, V. Buscaglia, Role of microstructures in the dielectric properties of PVDF-based nanocomposites containing high-permittivity fillers for energy storage, ACS Appl. Mater. Interfaces 15 (2023) 13535–13544, https://doi.org/10.1021/acsami.2c23013.

[28] S.S. Hota, D. Panda, R. Panda, S. Mishra, S. Choudhury, L. Biswal, R.N. P. Choudhary, A. Satapathy, Dielectric characteristics and energy storage capabilities of PVDF-based composite incorporating 2D GnP nanofiller, Results Eng. 26 (2025), https://doi.org/10.1016/j.rineng.2025.105593.

[29] A.A. Al-Muntaser, R.A. Pashameah, K. Sharma, E. Alzahrani, A.E. Tarabiah, Reinforcement of structural, optical, electrical, and dielectric characteristics of <scp>CMC</scp> / <scp>PVA</scp> based on <scp>GNP</scp> / <scp>ZnO</scp> hybrid nanofiller: nanocomposites materials for energy-storage applications, Int. J. Energy Res. 46 (2022) 23984–23995, https://doi.org/10.1002/er.8695.

[30] P. Dey, S. Bhattacharjee, D.K. Yadav, B.Z. Hmar, K. Gayen, T.K. Bhowmick, Valorization of waste biomass for synthesis of carboxy-methyl-cellulose as a sustainable edible coating on fruits: a review, Int. J. Biol. Macromol. 253 (2023) 127412, https://doi.org/10.1016/j.ijbiomac.2023.127412.

[31] E.M. Costa, S. Silva, A.R. Madureira, A. Cardelle-Cobas, F.K. Tavaria, M. M. Pintado, A comprehensive study into the impact of a chitosan mouthwash upon oral microorganism's biofilm formation in vitro, Carbohydr. Polym. 101 (2014) 1081–1086, https://doi.org/10.1016/j.carbpol.2013.09.041.

[32] Y.E. Rossi, S.M. Palacios, Insecticidal toxicity of Eucalyptus cinerea essential oil and 1,8-cineole against Musca domestica and possible uses according to the metabolic response of flies, Ind. Crop. Prod. 63 (2015) 133–137, https://doi.org/10.1016/j.indcrop.2014.10.019.

[33] J. Chen, G. Wu, Beetle forewings: epitome of the optimal design for lightweight composite materials, Carbohydr. Polym. 91 (2013) 659–665, https://doi.org/10.1016/j.carbpol.2012.08.061.

[34] B. Lyu, X. Duan, D. Gao, J. Ma, X.-Y. Hou, J. Zhang, Modified rapeseed oil/silane coupling agent-montmorillonite nanocomposites prepared by in-situ method: synthesis and properties, Ind. Crop. Prod. 70 (2015) 292–300, https://doi.org/10.1016/j.indcrop.2015.03.034.

[35] A. Wijayani, K. Ummah, S. Tjahjani, Characterization of carboxy methyl cellulose (CMC) from Eichornia crassipes (Mart) Solms, Indonesian, J. Chemother. 5 (2010) 228–231, https://doi.org/10.22146/ijc.21795.

[36] L. Wu, W. Wang, X. Zhang, X. Zhao, G. Yu, Anti-HBV activity and mechanism of marine-derived polyguluronate sulfate (PGS) in vitro, Carbohydr. Polym. 143 (2016) 139–148, https://doi.org/10.1016/j.carbpol.2016.01.065.

[37] P. Lemechko, E. Renard, G. Volet, C.S. Colin, J. Guezennec, V. Langlois, Functionalized oligoesters from poly(3-hydroxyalkanoate)s containing reactive end group for click chemistry: application to novel copolymer synthesis with poly (2-methyl-2-oxazoline), React. Funct. Polym. 72 (2012) 160–167, https://doi.org/10.1016/j.reactfunctpolym.2011.12.005.

[38] D. Guillén, S. Moreno-Mendieta, R. Pérez, C. Espitia, S. Sánchez, R. Rodríguez-Sanoja, Starch granules as a vehicle for the oral administration of immobilized antigens, Carbohydr. Polym. 112 (2014) 210–215, https://doi.org/10.1016/j.carbpol.2014.05.089.

[39] W. Tongdeesoontorn, L.J. Mauer, S. Wongruong, P. Sriburi, P. Rachtanapun, Effect of carboxymethyl cellulose concentration on physical properties of biodegradable

cassava starch-based films, Chem. Cent. J. 5 (2011) 6, https://doi.org/10.1186/1752-153X-5-6.
[40] M.M. Rahman, M. Alam, M.M. Rahman, M.A.B.H. Susan, Md.A.A. Shaikh, J. Nayeem, M.S. Jahan, A novel approach in increasing carboxymethylation reaction of cellulose, Carbohydr. Polym. Technol. Appl. 4 (2022) 100236, https://doi.org/10.1016/j.carpta.2022.100236.
[41] S.J. Park, S.Y. Lee, Systems biological approach for the production of various Polyhydroxyalkanoates by metabolically engineered *Escherichia coli*, Macromol. Symp. 224 (2005) 1–10, https://doi.org/10.1002/masy.200550601.
[42] H. Winkler, W. Vorwerg, R. Rihm, Thermal and mechanical properties of fatty acid starch esters, Carbohydr. Polym. 102 (2014) 941–949, https://doi.org/10.1016/j.carbpol.2013.10.040.
[43] K. Swennen, C. Courtin, B. Vanderbruggen, C. Vandecasteele, J. Delcour, Ultrafiltration and ethanol precipitation for isolation of arabinoxylooligosaccharides with different structures, Carbohydr. Polym. 62 (2005) 283–292, https://doi.org/10.1016/j.carbpol.2005.08.001.
[44] S.-J. Wu, J.-H. Wu, L.-Z. Xia, C. Chu, D. Liu, M. Gong, Preparation of xanthan-derived oligosaccharides and their hydroxyl radical scavenging activity, Carbohydr. Polym. 92 (2013) 1612–1614, https://doi.org/10.1016/j.carbpol.2012.11.016.
[45] J. Zhu, K. Zhang, Y. Zhang, C. Zhou, Z. Cui, W. Li, Y. Wang, J. Qin, Antioxidant hydrogel from poly(aspartic acid) and carboxymethylcellulose with quercetin loading as burn wound dressing, Int. J. Biol. Macromol. 282 (2024) 137323, https://doi.org/10.1016/j.ijbiomac.2024.137323.
[46] H. Li, H. Shi, Y. He, X. Fei, L. Peng, Preparation and characterization of carboxymethyl cellulose-based composite films reinforced by cellulose nanocrystals derived from pea hull waste for food packaging applications, Int. J. Biol. Macromol. 164 (2020) 4104–4112, https://doi.org/10.1016/j.ijbiomac.2020.09.010.
[47] M.-C. Popescu, B.-I. Dogaru, C.-M. Popescu, Effect of cellulose nanocrystals nanofiller on the structure and sorption properties of carboxymethyl cellulose–glycerol–cellulose nanocrystals nanocomposite systems, Materials 13 (2020) 2900, https://doi.org/10.3390/ma13132900.
[48] N.Y. Aldaleeli, M. Madani, S.A. Al-Gahtany, H. Elhaes, R. Badry, M.A. Ibrahim, Evaluation of different concentrations of graphene on the structural and optical properties of carboxymethyl cellulose sodium, Polymers (Basel). 17 (2025) 391, https://doi.org/10.3390/polym17030391.
[49] T. Churam, P. Usubharatana, H. Phungrassami, Sustainable production of carboxymethyl cellulose: a biopolymer alternative from sugarcane (*Saccharum officinarum* L.) leaves, Sustainability 16 (2024) 2352, https://doi.org/10.3390/su16062352.
[50] C. Cai, G. Wang, D. Xu, C. Yan, Production of dehydrated lignin-blending carboxylated nanocellulose with superior redispersion behavior and reinforcement effect for PVA nanocomposite films, Int. J. Biol. Macromol. 291 (2025) 139162, https://doi.org/10.1016/j.ijbiomac.2024.139162.
[51] N. Panchan, P. Wattanapan, S. Sungsinchai, S. Roddecha, P. Dittanet, A. Seubsai, C. Niamnuy, S. Devahastin, Optimization of synthesis conditions for carboxymethyl cellulose from pineapple leaf waste using microwave-assisted heating and its application as a food thickener, Bioresources 16 (2021) 7684–7701, https://doi.org/10.15376/biores.16.4.7684-7701.
[52] K. Fang, W. He, Y. Jiang, K. Li, J. Li, Preparation, characterization and physicochemical properties of cassava starch-ferulic acid complexes by mechanical activation, Int. J. Biol. Macromol. 160 (2020) 482–488, https://doi.org/10.1016/j.ijbiomac.2020.05.213.
[53] S. Silviana, M.C. Dzulkarom, Synthesis of cassava bagasse starch-based biocomposite reinforced woven bamboo fibre with lime juice as crosslinker and epoxidized waste cooking oil (EWCO) as bioplasticizer, J. Phys. Conf. Ser. 1295 (2019) 012076, https://doi.org/10.1088/1742-6596/1295/1/012076.
[54] K.S.V.P. Chandrika, A. Singh, R.D. Prasad, P. Yadav, M. Dhara, M. Kavya, A. Kumar, B. Gopalan, Porous crosslinked CMC-PVA biopolymer films: synthesis, standardization, and application in seed coating for improved germination, Carbohydr. Polym. Technol. Appl. 11 (2025) 100900, https://doi.org/10.1016/j.carpta.2025.100900.
[55] N. Karl, Charge carrier transport in organic semiconductors, Synth. Met. 133–134 (2003) 649–657, https://doi.org/10.1016/S0379-6779(02)00398-3.
[56] V. Cyriac, I.M. Ismayil, K. Noor, C. Mishra, R.F. Chavan, S.P. Bhajantri, Masti, ionic conductivity enhancement of PVA: carboxymethyl cellulose poly-blend electrolyte films through the doping of NaI salt, Cellulose 29 (2022) 3271–3291, https://doi.org/10.1007/s10570-022-04483-z.
[57] B. Wang, W. Huang, L. Chi, M. Al-Hashimi, T.J. Marks, A. Facchetti, High- *k* gate dielectrics for emerging flexible and stretchable electronics, Chem. Rev. 118 (2018) 5690–5754, https://doi.org/10.1021/acs.chemrev.8b00045.
[58] M.A. Morsi, E.M. Abdelrazek, R.M. Ramadan, I.S. Elashmawi, A. Rajeh, Structural, optical, mechanical, and dielectric properties studies of carboxymethyl cellulose/polyacrylamide/lithium titanate nanocomposites films as an application in energy storage devices, Polym. Test. 114 (2022), https://doi.org/10.1016/j.polymertesting.2022.107705.
[59] K. Gallegos-Rosas, A. Azari, C. Soldano, Carboxymethyl cellulose as a sustainable dielectric material for organic field-effect transistors, ACS Appl. Electron. Mater. 7 (2025) 1274–1282, https://doi.org/10.1021/acsaelm.4c02227.
[60] P. Martins, A.C. Lopes, S. Lanceros-Mendez, Electroactive phases of poly (vinylidene fluoride): determination, processing and applications, Prog. Polym. Sci. 39 (2014) 683–706, https://doi.org/10.1016/j.progpolymsci.2013.07.006.
[61] Q. Luo, H. Shen, G. Zhou, X. Xu, A mini-review on the dielectric properties of cellulose and nanocellulose-based materials as electronic components, Carbohydr. Polym. 303 (2023) 120449, https://doi.org/10.1016/j.carbpol.2022.120449.